

Solar Dynamo Model with Nonlocal Alpha-Effect

L. L. Kitchatinov^{1,2*}, S. V. Olemskoy¹

¹*Institute for Solar–Terrestrial Physics, Russian Academy of Sciences, Siberian Branch, P.O. Box 4026, Irkutsk, 664033 Russia*

²*Pulkovo Astronomical Observatory, Russian Academy of Sciences, Pulkovskoe sh. 65, St. Petersburg, 196140 Russia*

Abstract—The first results of the solar dynamo model that allows for the diamagnetic effect of inhomogeneous turbulence and the nonlocal alpha-effect due to the rise of magnetic loops are discussed. The nonlocal alpha-effect is not subject to the catastrophic quenching related to the conservation of magnetic helicity. Given the diamagnetic pumping, the magnetic fields are concentrated near the base of the convection zone, although the distributed-type model covers the entire thickness of the convection zone. The magnetic cycle period, the equatorial symmetry of the field, its meridional drift, and the polar-to-toroidal field ratio obtained in the model are in agreement with observations. There is also some disagreement with observations pointing the ways of improving the model.

DOI: 10.1134/S1063773711040037

Keywords: *Sun: activity, Sun: magnetic fields, stars: magnetic fields, MHD.*

INTRODUCTION

The scale of the flows responsible for the generation of large-scale solar magnetic fields is not small compared to the depth of the convection zone. This primarily applies to the cyclonic flows responsible for the so-called alpha-effect (Parker 1955; Vainshtein et al. 1980), particularly to its emergence during the formation of magnetic loops because of magnetic buoyancy (Caligari et al. 1995). Active regions on the Sun are believed to emerge when deep toroidal fields rise to the solar surface. In this case, Joy’s law holds: the leading sunspots of active regions are closer to the equator than the following ones (see, e.g., Obridko 1985; Howard 1996). Babcock (1961) noted that, as a consequence of this law, the magnetic fields of active regions must contribute to the general poloidal field of the Sun, i.e., to the emergence of the alpha-effect. Evidence for the presence of the alpha-effect of this type on the Sun has recently been obtained from observations (Dasi-Espuig et al. 2010). Since the toroidal fields are located in deep layers of the Sun and the poloidal fields that emerge as they rise are formed near the surface, the corresponding alpha-effect is not local (Dikpati and Charbonneau 1999).

Figure 1 illustrates this circumstance. The nonlocal alpha-effect is particularly interesting in connection with the problem of catastrophic quenching of the alpha-effect (Brandenburg and Subramanian 2005). Basically, the problem consists in the following. The generation of a poloidal field because of the alpha-effect gives rise to a large-scale field with magnetic helicity. In view of the conservation of helicity, helicity equal in magnitude and opposite in sign must appear in a small-scale magnetic field. In turn, the helical small-scale field contributes to the alpha-effect that is opposite in

*E-mail: kit@iszf.irk.ru

sign to the already existing alpha-effect. As a result, as the large-scale field grows, the alpha-effect disappears and the field generation stops. However, this takes place only for the local alpha-effect. If the original toroidal field and the generated poloidal field are separated in space, then no magnetic helicity emerges and there is no catastrophic quenching (see, however, Brandenburg and Käpylä 2007). In Fig. 1, there is no linkage of the magnetic flux tubes of the poloidal field and the original toroidal field that must be present for helical magnetic structures (Moffat 1978). In this paper, we propose a solar dynamo model with a nonlocal alpha-effect.

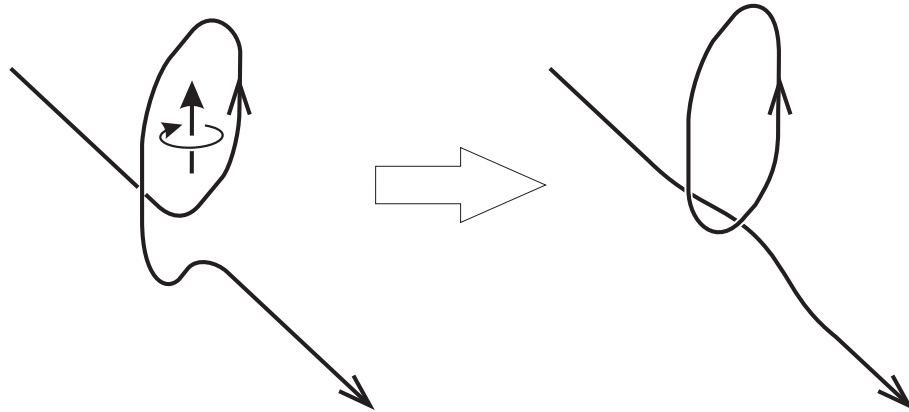


Fig. 1. Illustration of the emergence of the alpha-effect due to the rise of magnetic flux tubes. Under the action of the Coriolis force, the rising magnetic loop acquires a poloidal orientation. Reconnection at the loop footpoints disconnects it from the original magnetic flux tube of the toroidal field. The resulting toroidal and poloidal loops have no linkage and possess no magnetic helicity.

Another peculiarity of the proposed model is the concentration of the toroidal magnetic field near the base of the convection zone. This region is believed to be preferable for dynamo action (see, e.g., Gilman 1992). The dynamo models for the near-bottom region of the convection zone reproduce many features of the solar cycle (Parker 1993; Mason et al. 2008; Nefedov and Sokoloff 2010). However, the reasons why the magnetic field is concentrated in this region have not been specified. If the distributed-type model covers the entire thickness of the convection zone, then the magnetic field also turns out to be distributed over the entire thickness (Dikpati and Charbonneau 1999). In this paper, we take into account the diamagnetic effect of inhomogeneous turbulence, which leads to the field concentration near the bottom of the convection zone.

Turbulent conducting fluids expel large-scale magnetic fields into regions of space with a relatively low turbulence intensity (Zel'dovich 1956), i.e., turbulent conducting fluids possess diamagnetic properties with respect to large-scale fields. The presence of fluctuating magnetic fields had long been thought to suppress the diamagnetic effect of turbulence. However, both numerical (Dorch and Nordlund 2001; Brandenburg et al. 2010) and laboratory (Spence et al. 2007) experiments confirm its reality. The importance of this effect for the solar dynamo was pointed out in a number of papers (Ivanova and Ruzmaikin 1976; Krivodubskii 1984; Rüdiger and Brandenburg 1995; Guerrero and de Gouveia Dal Pino 2008). It is also important for the formation of the solar tachocline (Kitchatinov and Rüdiger 2008). Allowance for the diamagnetic pumping of the field in the dynamo model considered here provides the concentration of magnetic fields near the bottom of the convection zone.

The observed toroidal-to-poloidal field ratio suggests the presence of such a concentration on the Sun. The poloidal (polar) field has a strength of about 1–2 G. The toroidal fields are approximately

a factor of 1000 stronger if their strength is judged from the sunspot fields. The relative latitudinal inhomogeneity of the angular velocity is about 30%. Such rotation inhomogeneity can produce a toroidal field that is approximately a factor of 40 stronger than the existing poloidal field in 11 years (strong rotation inhomogeneity in the tachocline does not change this estimate, because the radial field component here must be smaller than the meridional one by the same factor by which the radial rotation inhomogeneity is larger than its latitudinal inhomogeneity). Therefore, the presence of poloidal fields with a strength of ~ 100 G is needed for the differential rotation to be able to produce toroidal fields with a strength of several thousand gauss during the solar cycle. The magnetic field concentration near the bottom of the convection zone in the proposed model provides the required poloidal field strength.

In this paper, we discuss the first results of the dynamo model that simultaneously allows for the diamagnetic pumping of the field and the nonlocal alpha-effect. In a number of parameters, the results show agreement with observations.

THE MODEL

The velocity of diamagnetic pumping of the field is related to the inhomogeneity of turbulent magnetic diffusivity η_T (Krause and Rädler 1980) by

$$\mathbf{U}_{\text{dia}} = -\frac{1}{2}\nabla\eta_T. \quad (1)$$

Given this pumping, the induction equation for large-scale fields can be written as

$$\frac{\partial\mathbf{B}}{\partial t} = \text{curl}\left(\mathbf{V}\times\mathbf{B} - \sqrt{\eta_T}\text{curl}(\sqrt{\eta_T}\mathbf{B}) + \mathcal{A}\right), \quad (2)$$

where \mathcal{A} allows for the contribution of the alpha-effect. In nonlocal formulation, it can be written as (Brandenburg et al. 2008)

$$\mathcal{A}(\mathbf{r}) = \int \alpha(\mathbf{r}, \mathbf{r}')\mathbf{B}(\mathbf{r}') d^3r'. \quad (3)$$

We will refine the form of the function $\alpha(\mathbf{r}, \mathbf{r}')$ below. The fluid velocity \mathbf{V} in (2) corresponds to (inhomogeneous) rotation,

$$\mathbf{V} = \mathbf{e}_\phi r \sin\theta \Omega f(r/R_\odot, \theta), \quad (4)$$

where the ordinary spherical coordinates (r, θ, ϕ) are used, Ω is the mean angular velocity, \mathbf{e}_ϕ is a unit vector in the azimuthal direction, $f(x, \theta)$ is the dimensionless rotation frequency, and $x = r/R_\odot$ is the relative radius. We will use the approximation of the helioseismological data on the Sun's inhomogeneous rotation proposed by Belvedere et al. (2000)

$$f(x, \theta) = \frac{1}{461} \sum_{m=0}^2 \cos\left(2m\left(\frac{\pi}{2} - \theta\right)\right) \sum_{n=0}^4 C_{nm} x^n. \quad (5)$$

The values of the coefficients C_{nm} are given in Table 1 from Belvedere et al. (2000). Figure 2 shows angular velocity isolines for the rotation specified in this way.

Let us consider a two-dimensional dynamo, i.e., we will assume the magnetic field to be cylindrically symmetric relative to the rotation axis:

$$\mathbf{B} = \mathbf{e}_\phi B + \text{curl}\left(\mathbf{e}_\phi \frac{A}{r \sin\theta}\right), \quad (6)$$

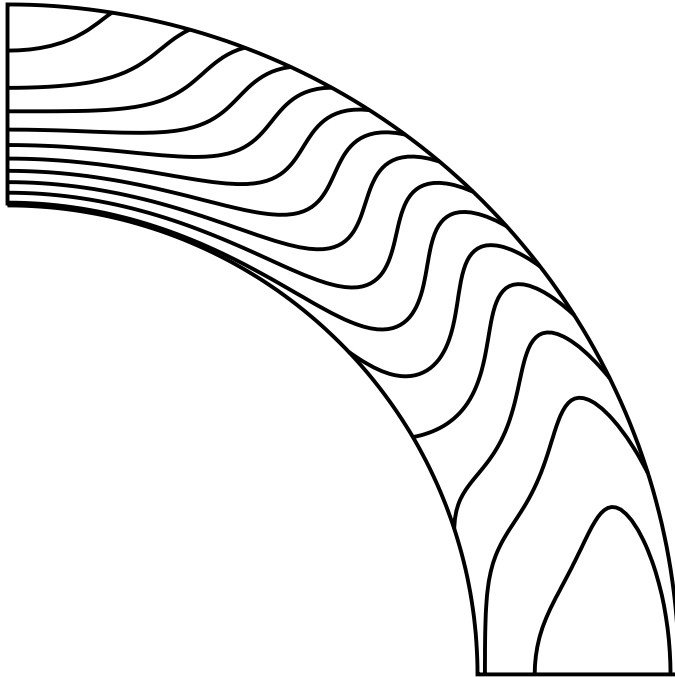


Fig. 2. Angular velocity isolines for the differential rotation used in the model. The angular velocity distribution is the approximation of the helioseismological data on the internal solar rotation (Belvedere et al. 2000).

where B is the toroidal magnetic field and A is the potential of the poloidal field. We will apply the $\alpha\Omega$ -dynamo approximation in which the generation of a toroidal field due to the alpha-effect is neglected (the toroidal field is generated by the differential rotation much more efficiently).

We use dimensionless variables: the time is measured in units of R_\odot^2/η_0 (η_0 is the characteristic turbulent diffusivity in the convection zone), the magnetic field is in units of the field strength B_0 for which the nonlinear effects are important, the function α is in units of α_0 (its characteristic amplitude), and the potential of the poloidal field is in units of $\alpha_0 B_0 R_\odot^3/\eta_0$. We will retain the previous notation for all of the normalized quantities, except for the relative radius $x = r/R_\odot$ and diffusivity $\eta = \eta_r/\eta_0$. The equation for the toroidal field in dimensionless variables will be written as

$$\begin{aligned} \frac{\partial B}{\partial t} &= \frac{\mathcal{D}}{x} \left(\frac{\partial f}{\partial x} \frac{\partial A}{\partial \theta} - \frac{\partial f}{\partial \theta} \frac{\partial A}{\partial x} \right) \\ &+ \frac{\eta}{x^2} \frac{\partial}{\partial \theta} \left(\frac{1}{\sin \theta} \frac{\partial(\sin \theta B)}{\partial \theta} \right) + \frac{1}{x} \frac{\partial}{\partial x} \left(\sqrt{\eta} \frac{\partial(\sqrt{\eta} x B)}{\partial x} \right), \end{aligned} \quad (7)$$

where

$$\mathcal{D} = \frac{\alpha_0 \Omega R_\odot^3}{\eta_0^2} \quad (8)$$

is the dynamo number that is the main controlling parameter of the model. We will write the equation for the poloidal field with the nonlocal alpha-effect as

$$\begin{aligned} \frac{\partial A}{\partial t} &= \frac{\eta}{x^2} \sin \theta \frac{\partial}{\partial \theta} \left(\frac{1}{\sin \theta} \frac{\partial A}{\partial \theta} \right) + \sqrt{\eta} \frac{\partial}{\partial x} \left(\sqrt{\eta} \frac{\partial A}{\partial x} \right) \\ &+ x \sin \theta \cos \theta \int_{x_i}^x \alpha(x, x') B(x', \theta) dx', \end{aligned} \quad (9)$$

where the integration is only over the radius and is bounded by the upper limit x . This qualitatively reflects the fact that the magnetic fields rising from deeper regions $x' < x$, contribute to the alpha-effect at some point x and the velocities of the rise deviate only slightly from the vertical direction. The alpha-effect due to the rise of magnetic loops was discussed in many papers, but the available results are not sufficient for its unambiguous quantitative allowance. It is necessary to invoke qualitative considerations. We will write the function $\alpha(x, x')$ from (9) as

$$\begin{aligned}\alpha(x, x') &= \frac{\phi_b(x')\phi_\alpha(x)}{1 + B^2(x', \theta)}, \\ \phi_b(x') &= \frac{1}{2} (1 - \operatorname{erf}((x' - x_i - 2.5h_b)/h_b)), \\ \phi_\alpha(x) &= \frac{1}{2} (1 + \operatorname{erf}((x - 1 + 2.5h_\alpha)/h_\alpha)),\end{aligned}\tag{10}$$

where x_i is the radius of the inner boundary of the distributed-type model, h_b and h_α are the numerical parameters of the model, and erf is the error function. The function $\phi_b(x')$ defines the (near-bottom) region whose toroidal fields produce the alpha-effect and the function $\phi_\alpha(x)$ describes the near-surface region in which this effect emerges. The quantity $1 + B^2$ in the denominator of (10) allows for the nonlinear suppression of the alpha-effect. Strong fields rise rapidly and the transformation of toroidal fields into poloidal ones due to the Coriolis force becomes inefficient. Similar views of the alpha-effect were used by Durney (1995), Dikpati and Charbonneau (1999), and Catterjee et al. (2004). The results discussed below were obtained for $x_i = 0.7$, $h_b = 0.002$, and $h_\alpha = 0.02$.

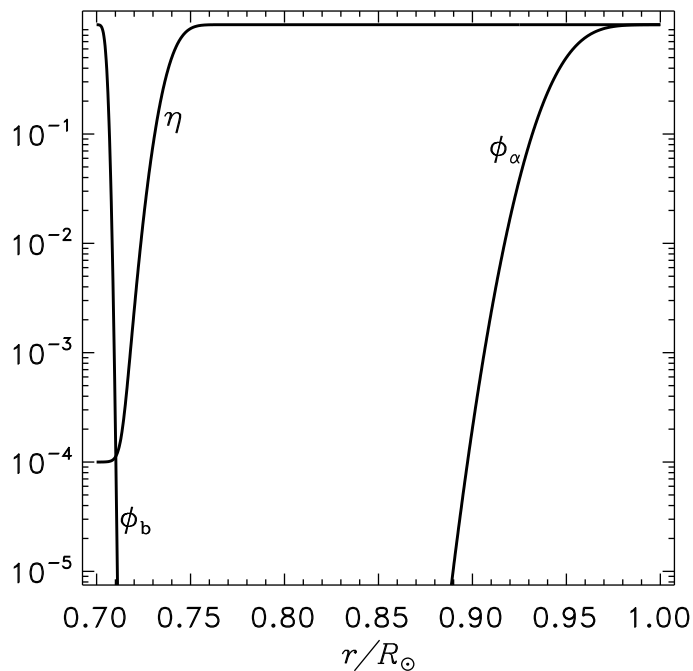


Fig. 3. Magnetic diffusivity profile, along with the functions ϕ_b and ϕ_α defining the nonlocal alpha-effect.

We use the following magnetic diffusivity distribution:

$$\eta(x) = \eta_{\text{in}} + \frac{1}{2} (1 - \eta_{\text{in}}) \left(1 + \operatorname{erf} \left(\frac{x - x_\eta}{h_\eta} \right) \right).\tag{11}$$

Figure 3 shows the magnetic diffusivity profile for the parameters adopted in our calculations ($\eta_{\text{in}} =$

10^{-4} , $x_\eta = 0.74$, $h_\eta = 0.01$), along with the functions ϕ_b and ϕ_α from Eq. (10) that define the nonlocal alpha-effect.

The conditions at the lower boundary correspond to the interface with a superconductor,

$$\frac{\partial(\sqrt{\eta}xB)}{\partial x} = 0, \quad A = 0, \quad x = x_i. \quad (12)$$

At the upper boundary, only the radial field component is nonzero (pseudo-vacuum boundary conditions):

$$B = 0, \quad \frac{\partial A}{\partial x} = 0, \quad x = 1. \quad (13)$$

The initial-value problem for the system of equations (7) and (9) was solved numerically. Since allowance for the diamagnetic pumping of the field leads to strong inhomogeneity of the solutions near the base of the convection zone, we used a radially nonuniform (and latitudinally uniform) grid. The grid spacing was $\Delta x \sim \sqrt{\eta}$. All of the results discussed below do not depend on the numerical resolution (this was checked by the repetition of calculations with doubled resolution).

Two types of symmetry of the solutions relative the equator are possible in linear dynamo problems: antisymmetric solutions, or dipolar modes, for which B and $\partial A/\partial\theta$ are antisymmetric relative to the equator ($B(\theta) = -B(\pi - \theta)$), and symmetric solutions, or quadrupolar modes ($B(\theta) = B(\pi - \theta)$). In nonlinear dynamo models (to which our model belongs), the solutions may not have a certain equatorial symmetry. Nevertheless, the symmetry of the solutions can be specified by additional boundary conditions on the equator. In most calculations, no equatorial symmetry was prescribed, but the solutions approached a certain type of symmetry after a sufficiently long calculation time. When it was required to determine the conditions for the excitation of symmetric or antisymmetric magnetic field modes, we applied the boundary conditions on the equator.

RESULTS AND DISCUSSION

The critical value of the dynamo number (8) for our model is $\mathcal{D}_c = 1.9 \times 10^4$. The field generation takes place for $\mathcal{D} > \mathcal{D}_c$. Fields antisymmetric relative to the equator are generated. The global solar magnetic field also belongs to this type of symmetry. To be more precise, only the antisymmetric component of the fields observed on the Sun exhibits an 11-year cyclicity (Stenflo 1988). The symmetric component is characterized by approximately a factor of 10 lower amplitude and by irregular variations with time. The critical dynamo number for the generation of symmetric modes ($\mathcal{D}_q = 2.5 \times 10^4$) is considerably larger than \mathcal{D}_c . The so obvious preference of dipolar modes is characteristic of dynamo models with a relatively low magnetic diffusivity near the base of the convection zone (Chatterjee et al. 2004).

In all likelihood, the reason is as follows. For modes with a dipolar equatorial symmetry, the spatial scale of the poloidal field (in latitude) is larger than that of the toroidal one. For quadrupole modes, the toroidal field has a larger scale. The poloidal field is distributed over the entire thickness of the convection zone, while the toroidal field is concentrated near its base, where the magnetic diffusion is small (Fig. 4). Therefore, the poloidal field is subject to the destructive action of magnetic diffusion to a greater extent and the (antisymmetric) modes whose poloidal field has a larger scale are generated more easily.

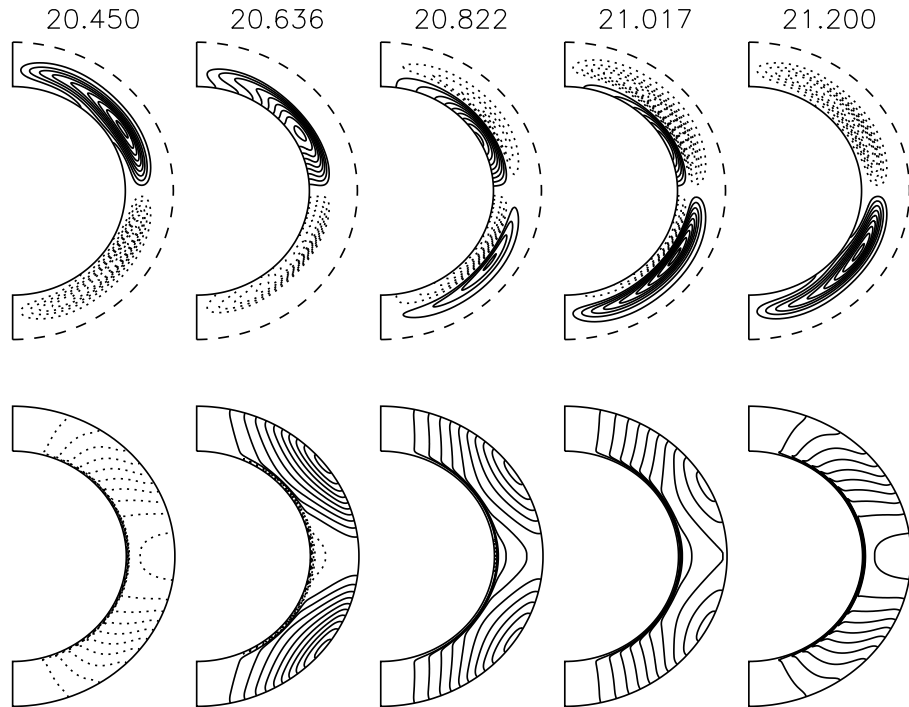


Fig. 4. Toroidal field isolines (top) and poloidal field lines (bottom) for several instants of one magnetic cycle. The time in dimensionless units (R_{\odot}^2/η_0) is shown in the upper part of the figure. The solid lines indicate positive levels and field lines with clockwise circulation, while the dotted lines indicate negative levels and counterclockwise circulation. In the upper row of graphs, the scale along the radius was changed in such a way that the dashed boundary corresponds to the radius $r = 0.74R_{\odot}$ below which the toroidal field is localized. The results of our calculations for $\mathcal{D} = 2.2 \times 10^4$ are shown.

Figure 4 shows the field distribution in the convection zone and its variations in the magnetic cycle. The strongest fields are concentrated near the bottom of the convection zone. In the model under consideration, such a concentration results from the diamagnetic pumping of the field (Zel'dovich 1956). However, the pumping does not affect the radial field component parallel to the pumping direction. Therefore, the poloidal field emerges on the outer surface. Nevertheless, the poloidal field reaches its largest strength near the lower boundary. That is why the differential rotation can generate fairly strong toroidal fields during the magnetic cycle. The polar field on the surface is approximately a factor of 1000 weaker than the characteristic toroidal field in our model. The period of the activity cycle (half the period of the full magnetic cycle) for Fig. 4 is about $0.75R_{\odot}^2/\eta_0$; for $\eta_0 \simeq 10^{13} \text{ cm}^2 \text{ s}^{-1}$, this gives a value close to the 11-year period of the solar cycle.

Figure 5 shows the calculated evolution of the field in latitude–time coordinates. For comparison with the butterfly diagram of sunspots, the toroidal field diagrams are usually constructed for some fixed depth. In the model under consideration, the toroidal field is concentrated in a thin near-bottom layer, where it strongly depends on the depth. Therefore, Fig. 5 shows a diagram for the depth-integrated toroidal field,

$$\mathcal{B}(\theta) = \sin \theta \int_{x_i}^1 B(x, \theta) x^2 dx. \quad (14)$$

The coefficient $\sin \theta$ in (14) allows for the latitude dependence of the length of the toroidal field flux tubes (the probability for the rise of magnetic loops with the formation of sunspots is assumed

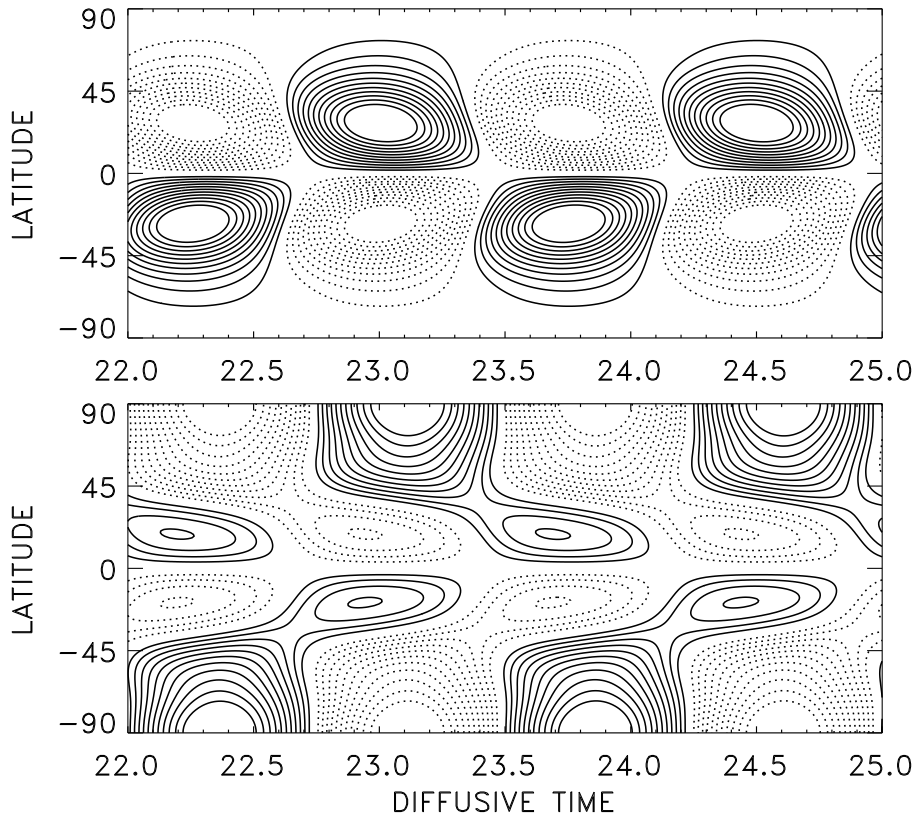


Fig. 5. Isolines of the depth-integrated toroidal magnetic field \mathcal{B} (top) and the radial magnetic field component on the surface (bottom) in latitude–time coordinates. The solid and dotted lines indicate positive and negative levels, respectively. The time is given in units of the diffusion time R_{\odot}^2/η_0 . The quantity \mathcal{B} is defined in (14).

to be proportional to the length of the magnetic flux tube).

The toroidal field diagram in Fig. 5 shows an equatorward drift during magnetic cycles. Note that the Yoshimura (1975) law is inapplicable for the nonlocal dynamo and the latitudinal drift is not related to the rotation inhomogeneity. The radial rotation inhomogeneity in our model is small and changes its sign depending on the latitude (Fig. 2).

The polar field in Fig. 5 changes its sign when the toroidal field reaches its largest strength, i.e., at the magnetic cycle maximum. The poloidal field diagram in this figure is close to that constructed by Obridko et al. (2006) from observational data and to the results by Stenflo (1988).

The presence of calculated toroidal fields at excessively high latitudes remains the only obvious disagreement of the proposed model with observations. The sunspot activity on the Sun is limited to equatorial latitudes, below approximately 30° . The toroidal field diagram in Fig. 5 covers a wider range of latitudes. It is hoped that this disagreement can be alleviated by taking into account the meridional flow. Near the base of the convection zone where the toroidal fields are localized, the meridional flow is directed equatorward and must lead to the field concentration near the equator. Another possibility for improving the model is to study the alpha-effect due to the rise of magnetic loops. Insufficient knowledge of this effect leads to certain arbitrariness (free parameters) in the model. At the same time, even in its simplest present-day version, the model is consistent with observations in a number of parameters (the cycle period, the equatorial symmetry, the relation between the amplitudes and signs of the toroidal and poloidal fields, the equatorial field drift), showing that it is

promising.

ACKNOWLEDGMENTS

This work was supported by the Russian Foundation for Basic Research (project nos. 10-02-00148 and 10-02-00391).

REFERENCES

- Babcock H.W.: 1961, ApJ **133**, 572.
- Belvedere G., Kuzanyan K.M., Sokoloff D.D.: 2000, MNRAS **315**, 778.
- Brandenburg A., Käpylä P.J.: 2007, New J. Phys. **9**, 305.
- Brandenburg A., Subramanian K.: 2005, Phys. Rep. **417**, 1.
- Brandenburg A., Rädler K.-H., Schrunner M.: 2008, A&A **482**, 739.
- Brandenburg A., Kemel K., Kleeorin N., Rogachevskii I.: 2010, arXiv:1005.5700.
- Caligari P., Moreno-Insertis F., Schüssler M.: 1995, ApJ **441**, 886.
- Chatterjee P., Nandy D., Choudhuri A.R.: 2004, A&A **427**, 1019.
- Dasi-Espuig M., Solanki S.K., Krivova N.A. et al.: 2010, A&A **518**, 7.
- Dikpati M., Charbonneau P.: 1999, ApJ **518**, 508.
- Dorch S.B.F., Nordlund Å.: 2001, A&A **365**, 562.
- Durney B.R.: 1995, Solar Phys. **160**, 213.
- Gilman P.A.: 1992, ASP Conf. Series **27**, 241.
- Guerrero G. and de Gouveia Dal Pino E.M.: 2008, A&A **485**, 267.
- Howard R.F.: 1996, Annu. Rev. Astron. Astrophys. **34**, 75.
- Ivanova T.S., Ruzmaikin A.A.: 1976, Astron. Zh. **53**, 398 [Sov. Astron. **20**, 227 (1976)].
- Kitchatinov L.L., Rüdiger G.: 2008, Astron. Nachr. **329**, 372.
- Krauze F., Rädler K.-H.: 1980, *Mean-Field Electrodynamics and Dynamo Theory* (Pergamon, Oxford; Mir, Moscow, 1984).
- Krivodubskii V.N.: 1984, Astron. Zh. **61**, 354 [Sov. Astron. **28**, 205 (1984)].
- Mason J., Hughes D.W., Tobias S.M.: 2008, MNRAS **391**, 467.
- Moffat H.K.: 1978, *Magnetic Field Generation in Electrically Conducting Fluids* (Cambridge Univ., London, New York; Mir, Moscow, 1980).
- Nefedov S.N., Sokoloff D.D.: 2010, Astron. Rep. **54**, 247.
- Obridko V.N.: 1985, *Sunspots and Activity Complexes* (Nauka, Moscow) [in Russian].
- Obridko V.N., Sokoloff D.D., Kuzanyan K.M., Shelting B.D., Zakharov V.G.: 2006, MNRAS **365**, 827.

Parker E.N.: 1955, ApJ **122**, 293.

Parker E.N.: 1993, ApJ **408**, 707.

Rüdiger G., Brandenburg A.: 1995, A&A **296**, 557.

Spence E.J., Nornberg M.D., Jacobson C.M. et al.: 2007, Phys. Rev. Lett. **98**, 4503.

Stenflo J.O.: 1988, Astrophys. Space Sci. **144**, 321.

Vainshtein S.I., Zel'dovich Ya.B., Ruzmaikin A.A.: 1980, *Turbulent Dynamo in Astrophysics* (Nauka, Moscow) [in Russian].

Yoshimura H.: 1975, ApJ **201**, 740.

Zel'dovich Ya.B.: 1956, JETP **4**, 460.

Translated by G. Rudnitskii